Adaptive Optics For Laser Space Debris Removal

Francis Bennet[a], Rodolphe Conan[a], Celine D'Orgeville[a], Murray Dawson[b], Nicolas Paulin[a], Ian Price[a], Francois Rigaut[a] Ian Ritchie[b], Craig Smith[b], Kristina Uhlendorf[a]

[a]Research School of Astronomy and Astrophysics, Australian National University, Mount Stromlo Observatory, Canberra, Australia

[b]EOS Space Systems, Mount Stromlo Observatory, Canberra, Australia

ABSTRACT

Space debris in low Earth orbit below 1500km is becoming an increasing threat to satellites and spacecrafts. Radar and laser tracking are currently used to monitor the orbits of thousands of space debris and active satellites are able to use this information to manoeuvre out of the way of a predicted collision. However, many satellites are not able to manoeuvre and debris-on debris collisions are becoming a significant contributor to the growing space debris population.

The removal of the space debris from orbit is the preferred and more definitive solution. Space debris removal may be achieved through laser ablation, whereby a high power laser corrected with an adaptive optics system could, in theory, allow ablation of the debris surface and so impart a remote thrust on the targeted object. The goal of this is to avoid collisions between space debris to prevent an exponential increase in the number of space debris objects.

We are developing an experiment to demonstrate the feasibility of laser ablation for space debris removal. This laser ablation demonstrator utilises a pulsed sodium laser to probe the atmosphere ahead of the space debris and the sun reflection of the space debris is used to provide atmospheric tip–tilt information. A deformable mirror is then shaped to correct an infrared laser beam on the uplink path to the debris. We present here the design and the expected performance of the system.

1. INTRODUCTION

The dawn of the space age in the late 1950's saw the launch of countless rockets into orbit around Earth. Associated with these early launches was the disposal of components in stable orbital configurations. Over time these components consisting of rocket bodies, old satellites, payload objects and associated items have accumulated in orbit. As the density of such objects increased the chance of collisions between larger objects grows. High orbital velocity and component construction results in any collision creating smaller fragments of space debris, which not only increases the chance of further collisions but also endangers operational satellites.[1]

A reliable and cost effective method for detecting and preventing collisions between orbital objects is required to prevent an exponential growth in the number of debris objects. EOS Space Systems have pioneered automated laser ranging of space debris objects, allowing detection of small objects (<10 cm) in low earth orbit, and larger objects to a range of 3000 km. Objects can be tracked with a ranging accuracy of 1.5 m in 0.1 s, achieving a prediction orbital accuracy of 200 m over 20 hours.[2] We present the development of an experiment to increase ranging precision and modify the orbit of space debris using a ground based adaptive optics (AO) corrected laser.

It has been suggested that a high power ground based laser system used in conjunction with a 10 m telescope could be used to modify the orbit of low mass space debris objects[3] for collision avoidance. Deorbiting of space debris has been considered with project ORION,[4] demonstrating that a MW class laser could be used to modify a stable orbit into a decaying orbit with a 5 m telescope and AO correction. Such a system was considered very costly at the time due to the high power and large fast slewing telescope required.

We propose a solution using a moderate power laser (10 kW) with a small (1.8 m), fast slewing telescope to track and modify the orbit of space debris. An AO system is used to correct the upward propagating beam in order to increase the precision of laser ranging, and to allow photon pressure to impart an orbital velocity change to avoid collisions.

Further author information: (Send correspondence to Rodolphe Conan)
Rodolphe Conan.: E-mail: rconan@mso.anu.edu.au

Adaptive Optics Systems III, edited by Brent L. Ellerbroek, Enrico Marchetti, Jean-Pierre Véran, Proc. of SPIE Vol. 8447, 844744 · © 2012 SPIE · CCC code: 0277-786/12/$18 · doi: 10.1117/12.925773

2. LASER RANGING AND ORBITAL MODIFICATION

Currently a pulsed laser operating at 1064 nm with 200 W average power is used to track and range space debris objects. The laser is propagated through the a 1.8 m telescope located on Mount Stromlo in Canberra, Australia. Object orbits are calculated using the ranging and tracking information, and checked with an automated tracking system.

The adaptive optic system presented here is under development to improve the ranging and tracking ability of the system. A 10 kW CW probe laser operating at 1064 nm is planned to be introduced into the system in conjunction with the AO system to provide photon pressure to modify the orbit of high area to mass ratio debris objects in orbit. The laser propagates through an AO corrected path to the telescope and on to the target.

An ideal scenario occurs when a target's orbit tracks directly overhead the laser station. In such a case the target can be acquired with minimal laser power as it rises over the horizon and tracked to zenith. At this point the probe laser power is increased to induce an orbital change due to added momentum of photon pressure. This high-power mode can be maintained until 70°zenith angle at which point either tracking is stopped or the laser power is reduced . The aim of adding momentum to the orbiting object is to modify the orbit, which is most efficiently done by adding or removing momentum in the object's direction of travel (Fig. 1). Increasing or decreasing orbital velocity is achieved between 10°and 70°zenith angle. Photon pressure is stopped at 70°due to increased altitude of the LGS reducing photon return, and increased turbulence in the atmosphere reducing AO performance.

We expect a high albedo object of diameter 50 cm (for example a sheet of thin Aluminium) to require less than 10 passes overhead to achieve a measured orbital shift of 100 m. The velocity change per overhead pass Δv_{pp} is calculated by integrating the imparted momentum in the direction of travel $\vec{A}$ between zenith angles Z 10°and 70°:

$$\Delta v_{pp} = \int_{10^\circ}^{70^\circ} \frac{(1 + R_{Al}) I(Z)}{\omega_S(Z) c M} \tau(Z) E_E \vec{A} \, dZ, \tag{1}$$

where R_{Al} is the reflectivity of the target material (Aluminium in this case), ω_S is the orbital angular velocity as seen from the launch station, c is the speed of light and M is the mass of the target. $\tau(Z)$ is the transmission through all optical elements and the atmosphere for zenith angle Z, and E_E is the ensquared energy of the probe beam on the target, and $I(Z)$ is the beam intensity on the target.

3. AO CORRECTION SYSTEM

An adaptive optic system is used to correct the upward propagating probe laser to improve the photon return for ranging and orbital modification.

3.1 Architecture

The AO system uses a Sodium laser guide star (LGS) to measure high order wavefront aberrations and reflection of sunlight from the target for tip-tilt measurements. The LGS is in front of the target 10" off axis. A cooled deformable mirror (DM) with tip-tilt stage is used to correct the upward propagation of the probe laser. Cooling of the DM and other optical elements is required due to the high power (10 kW CW) of the probe laser.

Photons from the LGS are captured by the telescope and passed through the optical system including the DM and a dichroic mirror to the LGS wavefront sensor (LGS WFS), and tip-tilt sensor (TTS) (Fig. 2). The probe laser source is projected through the same optical system, entering at the dichroic. The LGS WFS and TTS are connected to a realtime computer (RTC) for the computation of the wavefront and correction to be applied by the DM.

The full AO system architecture is shown in Fig. 3. The slopes from the LGS WFS computed by the RTC are used to correct high order aberrations and to correct the position of the LGS. The mean (tip and tilt) modes from the LGS WFS are passed through a low pass filter (LPF), and then sent to the LGS fast steering mirror

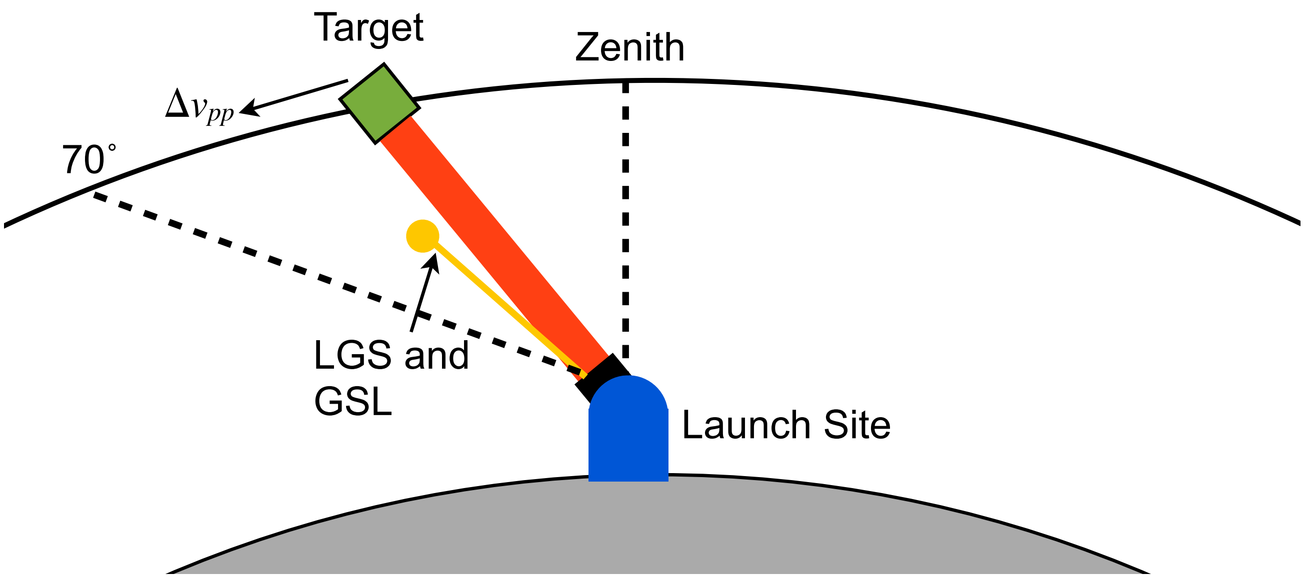

Figure 1. A probe laser (red line) launched from a ground based telescope to add momentum Δv_{pp} to a target in orbit passing directly overhead. A Sodium guide star laser (GSL) provides a LGS for measurement of high order wavefront aberrations. The high power laser tracks the target until 70°from zenith.

(LGS FSM) to correct the position on the LGS WFS of the LGS due to uplink propagation of the LGS. The LGS FSM operates at a frequency of 500 Hz.

The tip-tilt modes measured by the TTS are added to the LGS WFS modes after a calibration addressing any mismatch between the modes from each wavefront sensor. The slow tip and tilt modes (passed through another LPF) are sent to the tip-tilt stage (TT), and any remaining fast tip-tilt and high order modes are sent to the deformable mirror (DM) for correction. These corrections are subtracted from the incoming wavefront for the next iteration, and apply the correction to the upward propagating probe laser. The low pass filters are utilised to facilitate the different measurement and correction rates of each subsystem, the LGS WFS operating at 1.5 kHz, the TTS and FSM operating at 500 Hz.

3.2 Guide Star Laser

The guide star laser (GSL) is projected with a 30 cm diameter launch telescope, located 1 m from the telescope optical axis. The laser is a mode locked 589 nm pulsed laser operating with 100 MHz repetition rate with an average output power of 30 W. The launch telescope is steered to position the laser 10" ahead of the telescope optical axis, along the direction of travel.

3.3 Deformable Mirror

The DM to be used in this setup has a set of 20×20 cooled actuators in circular configuration with a diameter of 205 mm. The DM corrects all high order aberrations and contains a separate tip-tilt stage attached to the DM mount. The DM will operate at rates of up to 1.5 kHz, with the tip-tilt stage operating at around 50 Hz.

3.4 LGS WFS

The LGS WFS consists of an OCAM2 camera containing an E2V CCD 220 detector, with a 19×19 square lenslet array to form a Shack-Hartmann wavefront sensor. The sampling of each microlens in the array will be 6×6 pixels, and each subaperture corresponds to 9.4 cm of the full telescope aperture. The detector will operate at rates of up to 1.5 kHz when high photon return from the LGS is available, with readout noise of $<1e^-$.[5]

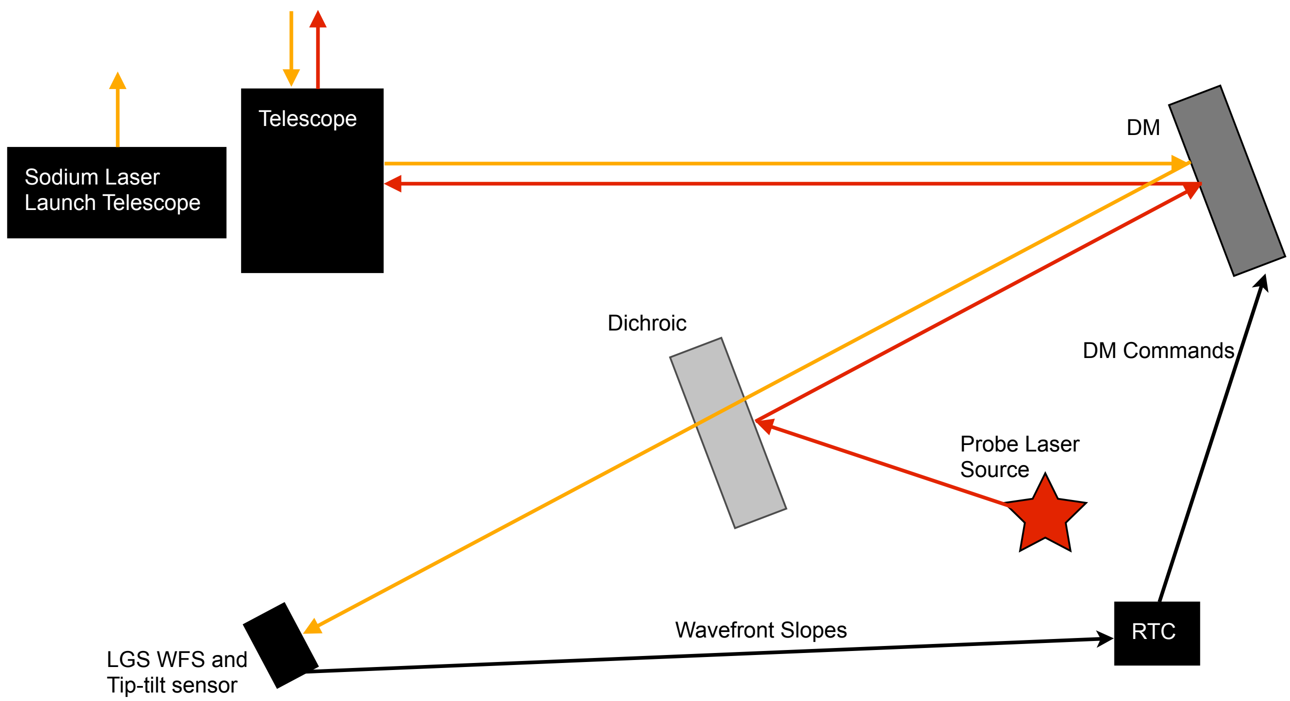

Figure 2. The ground based telescope collects light from the LGS launched through the Sodium laser launch telescope (orange line), and sunlight from the target, which is reflected off the DM and passes through a dichroic mirror to the LGS WFS. The information from these sensors is used to calculate the wavefront slopes, which are used to compute DM commands to correct the wavefront. The probe laser source projects its beam through the same optical path, undergoing correction by reflecting off the DM.

3.5 TTS

The TTS consists of a single imaging lens system and an Andor 860 camera. This camera with be used to capture the target for tracking and acquisition. Once the target is acquired it will switch to detecting tip-tilt from the reflected sunlight. A pixel area of 4×4 pixels will be used for tip-tilt centroiding. The TTS will operate at 500 Hz and will be combined with the LGS WFS slopes in the RTC to drive the DM and tip-tilt stage.

3.6 RTC

The real time computer (RTC) must compute all the elements required to operate the AO system. It receives pixel data from the LGS WFS and TTS, and processes this data into centroids in order to compute DM commands to correct the wavefront. Pixel data is converted to centroid measurements for each lenslet using a centre of gravity method. The calculated slopes from both sensors are combined and used to drive the DM and tip-tilt stage. Due to the high frame rate of the LGS WFS and DM the latency of such a system must be kept to a minimum. We require the total latency from image capture on the detector to DM actuation to be 125 μs. In order to achieve this large computing power is required (on the order of 7 GFLOPS) and low latency. This is achieved by using a custom PCIe FPGA based solution with separate inputs for the LGS WFS and TTS, and separate outputs for the DM and tip-tilt stage. The host PC will capture pixel data at a rate of 30 fps while the system is in operation, with the option to capture all frames for a short period of time. This data will be used for user interface displays, system analysis and monitoring.

4. EXPECTED AO PERFORMANCE

In this section we present the expected AO system performance based on numerical simulations run in MATLAB using the OOMAO API for adaptive optics *.

*Code available from R. Conan at https://github.com/rconan/OOMAO

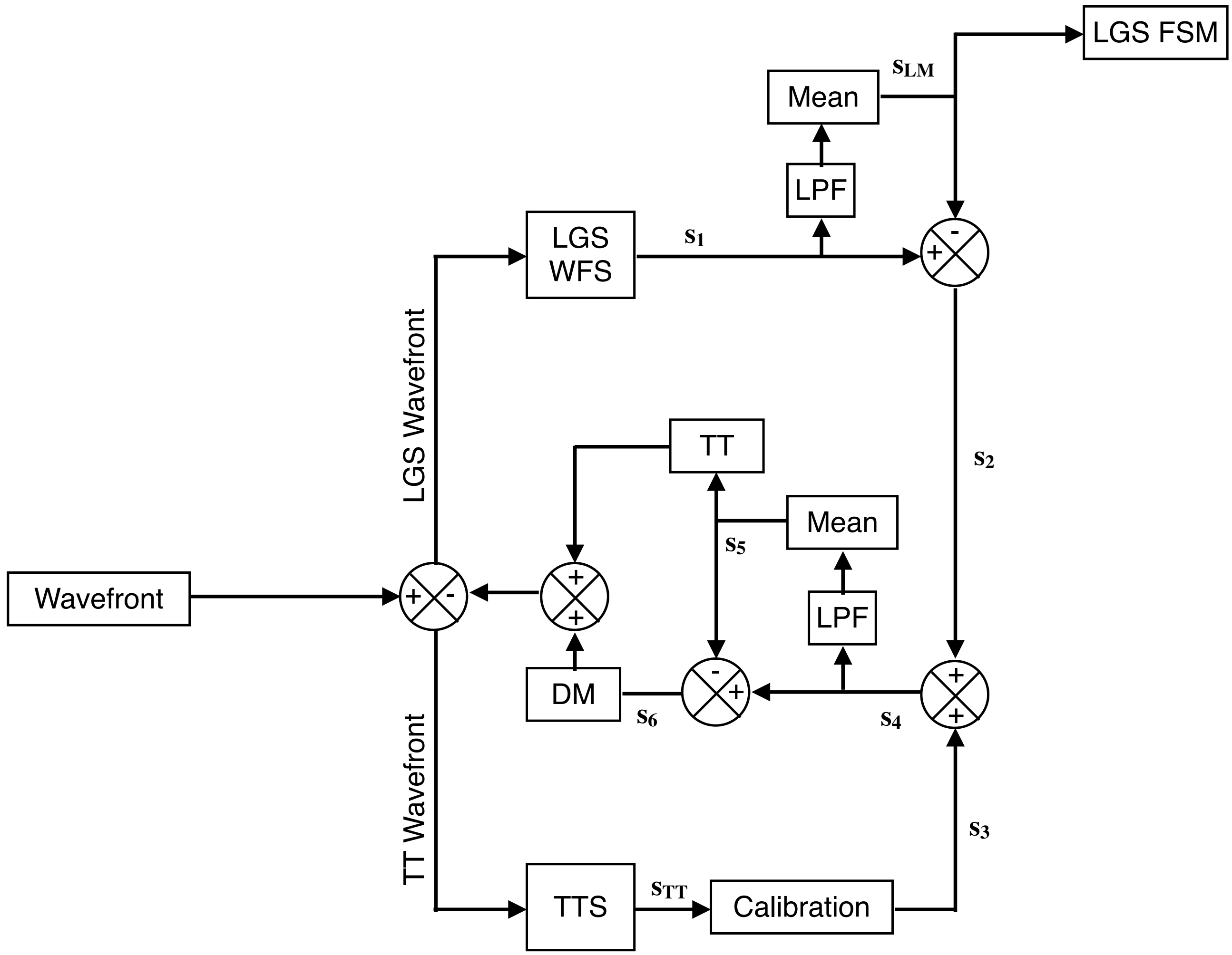

Figure 3. AO control block diagram.

4.1 Simulation Parameters

The atmospheric model consists of four atmospheric layers as shown in Table 1, with Fried parameter $r_0 = 10$ cm for a wavelength of 550 nm at zenith. The atmospheric model also takes into account the fast slewing speed of the telescope required to track an object in orbit. The sunlight reflected from the target used for tip-tilt correction has a magnitude of 7. The photon return from the LGS is 400 photons $\text{s}^{-1}\text{cm}^{-2}$.

Table 1. Atmospheric Turbulence Profile

Altitude (km)	Fractional r_0	Wind Speed	Wind Direction
0	0.4	10	0°
0.4	0.2	5	30°
6	0.3	60	0°
19	0.1	90	0°

The telescope is modelled as a single aperture with diameter 1.8 m, with a central obstruction ratio of 0.14:1. Simulations are run for a time of 0.1 seconds at zenith, sampling and correcting at 1.5 kHz. The readout noise and quantum efficiency of the LGS WFS are set to 0.5 and 0.9 respectively, and to 1 and 0.95 for the TTS.

We expect the AO system to result in a residual wavefront at 589 nm of 0.16 μm. The Strehl ratio at 1064 nm achieved is 0.7 with an ensquared energy of 0.24%.

REFERENCES

[1] Kessler, D. J. and Cour-Palais, B. G., "Collision Frequency of Artificial Satellites' The Creation of a Debris Belt," *Journal of Geophysical Research* **83**, 2637 (1978).

[2] Gao, Y., Smith, C., and Greene, B., "Laser Tracking of Space Debris," in [*European Space Surveillance Conference*], (2011).

[3] Mason, J., Stupl, J., Marshall, W., and Levit, C., "Orbital debrisdebris collision avoidance," *Advances in Space Research* **48**, 1643–1655 (Nov. 2011).

[4] Campbell, J., "Project ORION: orbital debris removal using ground-based sensors and lasers," *NASA Technical Memorandum* (108522) (1997).

[5] Mackay, C., Staley, T. D., King, D., Suess, F., and Weller, K., "High-speed, photon-counting CCD cameras for astronomy," *Proc. of SPIE* **7742**, 774202–1–11 (2010).